Me_3NO in accord with the observation that phosphite derivatives of metal carbonyl clusters react more slowly than expected relative to corresponding phosphine-type derivatives.

The differences in rates of reaction between $M_3(CO)_{12}$ and $M_3(CO)_{11}L$ for a given metal decrease in the order Fe > Ru > Os (Table V). This too can be explained in terms of the M-M bond length order of Fe-Fe < Ru-Ru < Os-Os,[5] which in turn mirrors the decreasing order of the inductive effect of L and thus the rates of reaction of $M_3(CO)_{11}L$. The complex $Fe_3(CO)_{11}L$ has two bridging carbonyls,[5] which may also enhance the effect of L on the reactivity of the CO groups. It is of interest to note that the difference in the rates of reaction between $Fe_3(CO)_{12}$ and $Fe_3(CO)_{11}L$ is as large as that between $M(CO)_6$ and $M(CO)_5L$,[8] where the nucleophilic attack on the monomeric metal carbonyls has to be on a CO coordinated to the same metal atom as L.

Acknowledgment. We wish to thank the United States-China Cooperative Science Program for the support of this collaborative research. The program is supported by the U.S. National Science Foundation and the PRC National Natural Science Foundation.

Supplementary Material Available: Table with additional rate data for the reactions under study (eq 2) and figures of IR and UV-vis absorbance changes versus reaction time (10 pages). Ordering information is given on any current masthead page.

Contribution from the Department of Chemistry and The Quantum Theory Project, University of Florida, Gainesville, Florida 32611

Electronic Causes of Dissymmetry in Side-On-Bonded Dioxygen Complexes

Thomas R. Cundari, M. C. Zerner,* and R. S. Drago*

Received December 21, 1987

The underlying reasons for the distortion of transition-metal tetraperoxides $M[O_2]_4^{n-}$ (M = Cr, n = 3; M = Mo, n = 2) are investigated. INDO/1 calculations are used. The method employed is to start with the symmetrical coordination mode (i.e. equal M-O bond lengths) and to look for significant differences in specific orbital interactions, which lead to the observed asymmetric geometry. Gradient optimization confirms the observation. The distortion is due to the greater interaction of the oxygen 2s orbitals (axial > equatorial) with the transition-metal p_z orbital. This interaction is made energetically feasible due to the high oxidation state of the metal and the negative charge on the peroxide fragment.

Introduction

Transition-metal peroxides are an important class of compounds in the oxidation of various organic substrates.[1,2] In particular, η^2-dioxygen complexes of group VIB metals have been used for epoxidations.[3,4] Theoretical investigations of this reaction have been reported.[5] In a number of these systems there exist small deviations of the dioxygen ligand from a symmetrical, isosceles triangle geometry.[6] This present research has sought electronic reasons for this dissymmetry in the particular case of metal tetraperoxides.

Since any mechanism of transition-metal η^2-peroxide catalyzed epoxidation[7,8] must involve the breaking of a metal-oxygen bond, differences in their strengths will have important implications in both the Sharpless[8] and Mimoun mechanisms.[7]

We have focused our attention on $Mo[O_2]_4^{2-}$ and $Cr[O_2]_4^{3-}$, which due to their reasonable size, high symmetry and large distortion from symmetrical coordination are ideal for this investigation (Figure 1). While there have been theoretical investigations[9-14] into the bonding of peroxides to metals, the reasons for the observed difference in metal-oxygen bond lengths in these complexes has never been fully addressed.

Table I. Geometrical Parameters[a,b]

metal	r(M-Oe)	r(M-Oa)	r(Oa-Oe)	∠(Oe-M-Oe')	∠(Oe-M-Oa)
Cr	1.958	1.882	1.466	175.37	44.83
Mo(obs)	2.000	1.930	1.546	177.20	46.30
Mo(calc)	1.97	1.92	1.24	179.4	37.0

[a] Taken from ref 9. [b] Distances in angstroms; angles in degrees.

Calculations

The INDO/1 semiempirical method was used.[15,16] Chromium tetraperoxide is an open-shell molecule, so the unrestricted Hartree-Fock formalism was used.[17] For molybdenum tetraperoxide a restricted wave function was used. Two sets of calculations were run on each molecule—at the experimentally determined geometries, given in Table I, and at a symmetrical geometry in which all the M-O bond lengths are equal to each other and the average of the observed bond length. Any important bonding interactions will be present in both. The bond order, overlap, Fock matrix elements, and atomic bond index are similar in both the symmetric and asymmetric geometries since the distortion is slight. The symmetrical configuration was studied in depth, and electronic causes for the geometric perturbation were investigated.

For two atomic orbitals to interact,[18] (1) they must overlap and (2) they must be of similar energy. A difference in the metal-oxygen in-

(1) Gubelmann, M. H.; Williams, A. F. *Structure and Bonding*; Springer-Verlag: Berlin, 1983; Vol. 55.
(2) Lyons, J. E. In *Aspects of Homogeneous Catalysis*; Ugo, R., Ed.; Reidel: Dordrecht, The Netherlands, 1977; Vol. 3.
(3) Mimoun, H. In *Comprehensive Inorganic Chemistry*, in press.
(4) Winter, W.; Mark, C.; Schurig, V. *Inorg. Chem.* **1980**, *19*, 2043.
(5) (a) Jørgensen, K. A.; Wheeler, R. A.; Hoffmann, R. *J. Am. Chem. Soc.* **1987**, *109*, 3240. (b) Jørgensen, K. A.; Hoffmann, R. *Acta Chem. Scand.* **1986**, *B40*, 411. (c) Purcell, K. *Organometallics* **1985**, *4*, 509.
(6) (a) Halpern, J. A.; Goodall, B. A.; Khare, J. P.; Lim, H. S.; Pluth, J. J. *J. Am. Chem. Soc.* **1975**, *97*, 2301. (b) Terry, N. W.; Amma, E. L.; Vaska, L. *J. Am. Chem. Soc.* **1972**, *94*, 653.
(7) Mimoun, H.; Seree de Roch, I.; Sajus, L. *Tetrahedron* **1970**, *26*, 37.
(8) Sharpless, K. B.; Townsend, J. M.; Williams, D. R. *J. Am. Chem. Soc.* **1972**, *94*, 295.
(9) Roch, M.; Weber, J.; Williams, A. F. *Inorg. Chem.* **1984**, *23*, 4571.
(10) Brown, D. H.; Perkins, R. H. *Inorg. Chim. Acta* **1974**, *8*, 285.
(11) Dacre, P. D.; Elder, M. *J. Chem. Soc., Dalton Trans.* **1972**, 1426.
(12) Fischer, J.; Veillard, A.; Weiss, R. *Theor. Chim.* Acta **1972**, *24*, 317.
(13) Rosch, N.; Hoffmann, R. *Inorg. Chem.* **1974**, *13*, 2656.
(14) Swalen, J. D.; Ibers, J. A. *J. Chem. Phys.* **1962**, *37*, 17.
(15) (a) Bacon, A. D.; Zerner, M. C. *Theor. Chim. Acta* **1979**, *53*, 21. (b) Andersen, W.; Edwards, W. D.; Zerner, M. C. *Inorg. Chem.* **1986**, *25*, 2728.
(16) Pople, J. A.; Beveridge, D. L. *Approximate Molecular Orbital Theory*; McGraw-Hill: New York, 1970.
(17) Pople, J. A.; Nesbet, R. K. *J. Chem. Phys.* **1954**, *22*, 571.
(18) (a) Whangbo, M-H.; Burdett, J.; Albright, T. *Orbital Interactions in Chemistry*; Wiley: New York, 1970. (b) Whangbo, M.-H.; Schlegel, H. B.; Wolfe, S. *J. Am. Chem. Soc.* **1977**, *99*, 1296.

0020-1669/88/1327-4239$01.50/0

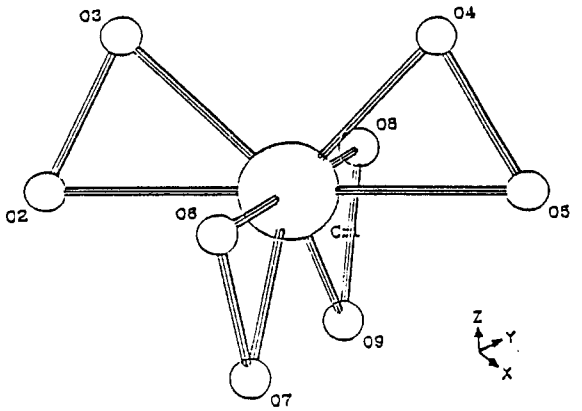

Figure 1. Geometry of transition-metal tetraperoxides.

teractions, for the symmetry-inequivalent oxygens, will manifest itself in the observed dissymmetry.

Four quantum chemical properties were compared for the analogous equatorial and axial oxygen AO's.

The first property is overlap, $S_{uv} = \langle \varphi_u | \varphi_v \rangle$. As the overlap increases the interaction between the two orbitals involved becomes stronger.

The bond order, P_{uv}, is defined as in eq 1, where C_{ui} and C_{vi} are the LCAO–MO coefficients of the AO's φ_u and φ_v in MO_i. The bond order

$$P_{uv} = 2\sum_{i}^{occ} C_{ui}C_{vi} \tag{1}$$

measures the extent to which the two AO's participate in the same occupied MO's and thus is indicative of energy match. A large positive value denotes a stabilizing interaction, and a large negative value denotes a destabilizing interaction.

Frontier orbital reasoning gives the energy of interaction of two AO's as[19]

$$E \propto \frac{F_{uv}^2}{E_u - E_v} \tag{2}$$

where F_{uv} is the appropriate Fock matrix element. A strong interaction has a large F_{uv}.

The atomic bond index between atoms A and B is defined as

$$B_{AB} = \sum_{u}^{\text{on A}} \sum_{v}^{\text{on B}} P_{uv}P_{vu} \tag{3}$$

where P_{uv} is the orbital bond order defined in eq 1, and the summations are over all AO's φ_u and φ_v on atoms A and B, respectively. The atomic bond index has the advantage of being rotationally invariant (the others are not) and yields a value of 1 for a single bond, 2 for a double bond, etc.

Point charges were included at sites occupied by counterions in the solid in order to simulate the local neutrality of the crystal lattice.[12,20] This led to a substantial improvement in the SCF convergence of the calculations. All occupied orbitals had eigenvalues less than or close to zero, representing ions stable to further ionization. An energy minimization starting with the symmetric structure was carried out on the molybdenum compound. Convergence was assumed when the maximum component of the gradient was less than 1×10^{-5} au. Since the axial and equatorial oxygens are not symmetry equivalent even with the symmetric geometry, this optimization led directly to a structure similar to that which is observed (Table I). As the symmetric structure does not represent a stationary point on the potential energy surface, it is not possible to compare the energy of the optimized asymmetric structure with an artifically constructed symmetric structure.

Results and Discussion

The orbital splitting diagram for a D_{2d}, eight-coordinate, dodecahedral complex is given in Figure 2. The unpaired electron in the d^1 chromium analogue is located in an orbital that is largely $d_{x^2-y^2}$ in character in agreement with previous theoretical[9,11] and experimental[21] work. The atomic bond index indicates a single bond between the two bonded oxygen atoms, even though the calculated bond lengths are shorter than those observed (1.466 and 1.546 Å for the chromium and molybdenum species,[9] respectively) i.e. they are peroxide-like in nature. This explains the long O–O bond that is experimentally determined for these compounds.

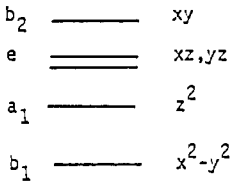

Figure 2. d-Orbital splitting for D_{2d} $M(O_2)_4^{n-}$

Table II. Overlap Matrix Elements in $Cr(O_2)_4^{3-}$ [a,b]

metal AO	axial oxygen AO				equatorial oxygen AO			
	2s	$2p_x$	$2p_y$	$2p_z$	2s	$2p_x$	$2p_y$	$2p_z$
4s	0.27	0.06	0.06	0.08	0.27	0.07	0.07	0.00
$4p_x$	0.20*	0.06	0.06	0.09	0.29*	0.01	0.13	0.01
$4p_y$	0.20*	0.06	0.06	0.09	0.29*	0.13	0.01	0.01
$4p_z$	0.30*	0.09	0.09	0.02*	0.02*	0.01	0.01	0.12*
$3d_{z^2}$	0.04	0.05	0.05	0.01	0.06	0.04	0.04	0.01
$3d_{x^2-y^2}$	0.00	0.03	0.03	0.00	0.00	0.04	0.04	0.00
$3d_{xy}$	0.05	0.01	0.01	0.06	0.11	0.08	0.08	0.01
$3d_{xz}$	0.08	0.01	0.06	0.06	0.01	0.00	0.01	0.04
$3d_{yz}$	0.08	0.06	0.01	0.06	0.01	0.01	0.00	0.04

[a] Symmetrical geometry. [b] Those differing to a significant degree ($\Delta S \geq 0.09$) are denoted with an asterisk.

Table III. Overlap Matrix Elements in $Mo[O_2]_4^{2-}$ [a,b]

metal AO	axial oxygen AO				equatorial oxygen AO			
	2s	$2p_x$	$2p_y$	$2p_z$	2s	$2p_x$	$2p_y$	$2p_z$
5s	0.27	0.04	0.04	0.06	0.27	0.06	0.06	0.00
$5p_x$	0.20*	0.07	0.05	0.08	0.29*	0.01	0.11	0.00
$5p_y$	0.20*	0.05	0.07	0.08	0.29*	0.11	0.01	0.00
$5p_z$	0.31*	0.08	0.08	0.00*	0.01*	0.00	0.00	0.12*
$4d_{z^2}$	0.06	0.06	0.06	0.01	0.09	0.06	0.06	0.01
$4d_{x^2-y^2}$	0.00	0.04	0.04	0.00	0.00	0.06	0.06	0.00
$4d_{xy}$	0.07	0.00*	0.01*	0.00	0.15	0.10*	0.10*	0.01
$4d_{xz}$	0.11*	0.01	0.07	0.07	0.01*	0.00	0.01	0.06
$4d_{yz}$	0.11*	0.07	0.01	0.07	0.01*	0.01	0.00	0.06

[a] Symmetrical geometry [b] Overlaps that differ by a significant amount ($\Delta S \geq 0.09$) are denoted by an asterisk.

Overlap. For the equatorial and axial oxygen atoms in chromium tetraperoxide there are four pairs of overlap integrals between the oxygen and the metal AO's which differ to a significant extent in their magnitude. For the molybdenum analogue there are five such pairs. These are given for $Cr(O_2)_4^{3-}$ in Table II and $Mo(O_2)_4^{2-}$ in Table III. The main difference is in the oxygen 2s orbitals and their overlap with the metal $4p_z$ or $5p_z$ AO's. This is easy to visualize in terms of the nodal properties of the metal p_z orbital. The equatorial oxygens lie near the nodal plane of the p_z orbital while the axial oxygens are positioned so that the 2s orbital can overlap with the p_z orbital of the metal.

Bond Order. When the bond orders for axial and equatorial oxygens in symmetrical chromium tetraperoxide are compared, it is found that the only pair of orbitals that differ in both overlap and bond order is the 2s and its interaction with the $4p_z$ metal AO's. The bond order between the O 2s and Cr $4p_z$ orbitals is 0.216, indicating a strong interaction for the axial oxygen, and for the equatorials it is −0.016, indicating a weakly antibonding interaction. For molybdenum the analogous bond orders are 0.253 (Mo $5p_z$–Oa 2s) and −0.020 (M $5p_z$–Oe 2s). It may seem counterintuitive that low-lying oxygen 2s orbitals would have a reasonable energy match with a metal p_z. The high oxidation state of Cr(V) and Mo(VI) leads to low-energy metal AO's and the negative charge on the peroxide fragment increases the energy of the oxygen AO's, leading to reasonable energy match. That the bond order is of such significant magnitude is convincing evidence. If there were not a good energy match between the oxygen 2s and the metal $4p_z$ or $5p_z$ orbitals they would not par-

(19) Jørgensen, K. A.; Hoffmann, R. *J. Am. Chem. Soc.* **1986**, *108*, 1867.
(20) Stomberg, R. *Acta Chem. Scand.* **1969**, *23*, 2755.
(21) Dalal, N. S.; Millar, J. M.; Jagadeesh, M. S.; Seehra, M. S. *J. Chem. Phys.* **1981**, *74*, 1916.

Table IV. Mulliken Population Analysis

metal AO	sym Mo	sym Cr	unsym Mo	unsym Cr
s	0.16	0.25	0.16	0.25
p_x	0.11	0.18	0.12	0.19
p_y	0.11	0.18	0.12	0.19
p_z	0.25	0.38	0.22	0.36
d_{z^2}	0.85	0.73	0.84	0.73
$d_{x^2-y^2}$	0.52	1.05	0.51	1.05
d_{xy}	0.73	0.47	0.73	0.46
d_{xz}	0.84	0.81	0.84	0.80
d_{yz}	0.84	0.81	0.84	0.80

ticipate in the same occupied MO's. A Mulliken population analysis (Table IV) reveals that the p_z orbital has a significantly higher population than the corresponding p_x and p_y orbitals. The calculations indicate that these changes in energy are of sufficient magnitude to cause substantial interaction.

Fock Matrix Elements. Comparing the Fock matrix elements between the equatorial and axial oxygen AO's and the metal AO's, we observe a large dissimilarity only for the oxygen 2s orbitals and the metal p_z orbitals. For chromium tetraperoxide F_{uv}(eq) = −0.015 and F_{uv}(ax) = −0.412 for the metal p_z and oxygen 2s orbitals. For molybdenum tetraperoxide similar differences are observed. this, once again, indicates a significant difference in the strength of the interaction between the axial and oxygen 2s AO's and the metal p_z orbital. The greater interactions (S_{uv}, P_{uv}, and F_{uv}) will lead to geometric distortions in the direction observed experimentally. No other orbital interactions satisfy the criterion of large differences for these three properties.

Atomic Bond Index. A comparison of the atomic bond indices between the symmetric and asymmetric structures is informative in that it is a summation of the various orbital interactions (and thus different from the previous three criterion) for the two atoms. Perturbation of the chromium tetraperoxide from the symmetric to asymmetric configuration leads to a small change in the chromium–equatorial oxygen bond index, from 0.66 to 0.65. However, the analogous chromium–axial oxygen bond index changes more substantially from 0.65 in the symmetric form to 0.69 in the asymmetric. For $Mo(O_2)_4^{2-}$ the changes are inconclusive since the differences are smaller and cancel each other out. Thus, at least for chromium the calculations indicate that the potential energy surface is softer for chromium–equatorial oxygen bond distortion than chromium–axial oxygen bond distortion. Thus, the chromium–axial oxygen bond can be distorted in a way that will increase its strength, with relative disregard for the chromium–equatorial oxygen bond, which is insensitive to this distortion mode. The weaker interactions of the equatorial oxygen atoms with the central metal atom, which we have pointed out throughout this paper, would seem to dictate just such a soft potential energy surface for this distortion.

Jahn–Teller Mechanism. We discounted a first-order Jahn–Teller distortion since no partially filled degenerate MO's exist in chromium tetraperoxide and the molybdenum analogue is a closed-shell molecule. A second-order Jahn–Teller distortion was deemed to be inoperative due to the presence of a good HOMO–LUMO gap, and the gap was rather insensitive to the geometrical distortion.

Finally, we note that the INDO calculations are approximate. Nevertheless they do produce a distortion of the bonding as observed in experiments. Furthermore, they provide a reasonable explanation for this distortion.

Conclusions

The difference between metal–oxygen bond lengths in molybdenum and chromium tetraperoxide is due in large part to the difference in the strength of interaction between the 2s AO's of axial and equatorial oxygen atoms with the metal p_z AO. Poorer overlap for the equatorial 2s orbitals combined with a much larger bond order for the axial 2s orbitals leads to a stronger interaction and provides the driving force for the ensuing distortion to dissymmetric coordination. A good energy match between the metal p_z and oxygen 2s orbitals is obtained due to the high oxidation state of the metal lowering its AO's while the negative charge on the peroxide raises the energy of its orbitals. A large bond order, significant population of the metal p_z orbital, and the Fock matrix elements all point to a reasonable energy match involving the metal p_z orbital. Additionally, a comparison of the change in atomic bond index as the distortion occurs indicates that the Cr–Oe bond is insensitive while the Cr–Oa bond strengthens more significantly.

Acknowledgment. Helpful discussions with A. Cameron and D. Swieter of the University of Florida are gratefully acknowledged. This work was supported in part through U.S. Army Research Center Grant No. DAAA15-85-C-0034.

Contribution from the Department of Chemistry, Auburn University, Auburn, Alabama 36849

Theoretical Study of the Interaction of NH_3 with the Boron Hydrides BH_3, B_3H_7, B_4H_8, and B_5H_9 and the Carboranes $C_2B_3H_5$ and $C_2B_3H_7$

Michael L. McKee

Received June 27, 1988

Geometries and energies of Lewis base adducts of ammonia with several boron hydrides and carboranes have been calculated by ab initio methods. Geometries were optimized at the HF/3-21G level, and single-point calculations were made at the MP2/6-31G* level. The B–N bond strength is largest when NH_3 is coordinated to a BH_2 unit that forms a three-center two-electron bond to the remainder of the molecule. A weaker B–N bond results when the BH_2 unit forms another two-center two-electron bond, while the weakest B–N bond occurs when the NH_3 is coordinated to a boron center that is already coordinatively rich.

Nucleophiles are known to form adducts with boron hydrides[1–3] and to a lesser extent with carboranes.[4,5] For the reactive boron hydrides B_3H_7 and B_4H_8, the structures of the free boron hydrides are often assumed to be the same as those of their adducts, since the former have not been isolated. However, the geometries of many adducts are radically different from the unadducted form

(1) Greenwood, N. N. In *Comprehensive Inorganic Chemistry*; Trotman-Dickenson, A. F., Ed.; Pergamon: New York, 1973; Vol. 3.
(2) Shore, S. G. *Pure Appl. Chem.* **1977**, *49*, 717–732 and reference cited therein.
(3) Fehlner, T. P.; Housecroft, C. E. In *Molecular Structures and Energetics*; Liebman, J. F., Greenberg, A., Eds.; Verlag Chemie International: Deerfield Beach, FL, 1984; Vol. 1.
(4) Onak, T. In *Comprehensive Organometallic Chemistry*; Wilkinson, G., Stone, F. G. A., Abel, E., Eds.; Pergamon: Oxford, England, 1982; Vol. 1, pp 411–457.
(5) Lew, L.; Haran, G.; Dobbie, R.; Black, M.; Onak, T. *J. Organomet. Chem.* **1976**, *111*, 123–130.

0020-1669/88/1327-4241$01.50/0